

Supporting Information for:

Retarded translocation of nucleic acids through α -hemolysin nanopore in the presence of a calcium flux

Sha Wang,^{#ab} Yuqin Wang,^{#ab} Shuanghong Yan,^{ab} Xiaoyu Du,^{ab} Panke Zhang,^a Hong-Yuan Chen^{*a} and Shuo Huang^{*ab}

[a] State Key Laboratory of Analytical Chemistry for Life Sciences, School of Chemistry and Chemical Engineering, Nanjing University, 210023, Nanjing, China

[b] Chemistry and Biomedicine Innovation Center (ChemBIC), Nanjing University, 210023, Nanjing, China

These authors contributed equally to this work

Corresponding Authors:

Prof. Hong-Yuan Chen: hychen@nju.edu.cn

Prof. Shuo Huang: shuo.huang@nju.edu.cn

Contents

Materials	3
Figure S1. A DIB device.	4
Figure S2. I-V curves of α -HL with different buffer combinations.	5
Figure S3. τ_{off} and τ_{on} of Let-7a translocation.....	6
Figure S4. τ_{off} and τ_{on} of poly(dA) ₂₃ and poly(rA) ₂₃	7
Figure S5. Electrophysiology measurements with CaCl ₂ in <i>cis</i>	8
Figure S6. Reverse potential measurement.	9
Figure S7. Retarded nucleic acid translocation in the presence of a calcium flux.....	10
Figure S8. Reduced threshold voltage.	11
Figure S9. Translocation of RNA homopolymers under different conditions.	12
Figure S10. Simultaneous detection of RNA homopolymers.....	13
Table S1. Strand sequences.	14
Table S2. τ_{off} and τ_{on} of poly(dA) ₂₃ in different buffer combinations.	14
Table S3. τ_{off} and τ_{on} of poly(rA) ₂₃ in different buffer combinations.	14
Table S4. The ratio of effective translocation for RNA homopolymers.	14
Table S5. τ_{off} and τ_{on} of RNA homopolymers translocation.	15

Materials

Pentane, hexadecane, silicone oil AR20, ethylenediaminetetraacetic acid (EDTA), Triton X-100 were purchased from Sigma-Aldrich. 1,2-diphytanoyl-sn-glycero-3-phosphocholine (DPhPC) was supplied by Avanti Polar Lipids. Fluo-8H sodium electrolyte (Fluo-8) was from AAT Bioquest. 4-(2-hydroxyethyl)-1-piperazine ethanesulfonic acid (HEPES) was from Shanghai Yuanye Bio-Technology (China). Potassium chloride, calcium chloride, sodium chloride, sodium hydrogen phosphate and sodium dihydrogen phosphate were obtained from Aladdin. Chelex 100 resin (biotechnology grade, 100-200 mesh, sodium form), Precision Plus Protein™ Dual Color Standards and TGX™ FastCast™ Acrylamide Kit (12%) were from Bio-Rad. Dioxane-free isopropyl-β-D-thiogalactopyranoside (IPTG), ampicillin sodium and imidazole, trimethylamine methane (tris), glycine and sodium dodecyl sulfate (SDS) were from Solarbio. *E. coli* strain BL21 (DE3) were from Biomed. Luria-Bertani (LB) broth and LB agar were from Hopebio (China). Hydrochloric acid (HCl) was from Sinopharm (China). All the items listed above were used as received.

MicroRNA (Let-7a) was custom synthesized by Genscript (New Jersey, USA). DNA and RNA homopolymers (**Table S1**) were custom synthesized by Sangon Biotechnology (Shanghai, China). All above nucleic acid samples were purified by high-performance liquid chromatography (HPLC) and used without any further purifications.

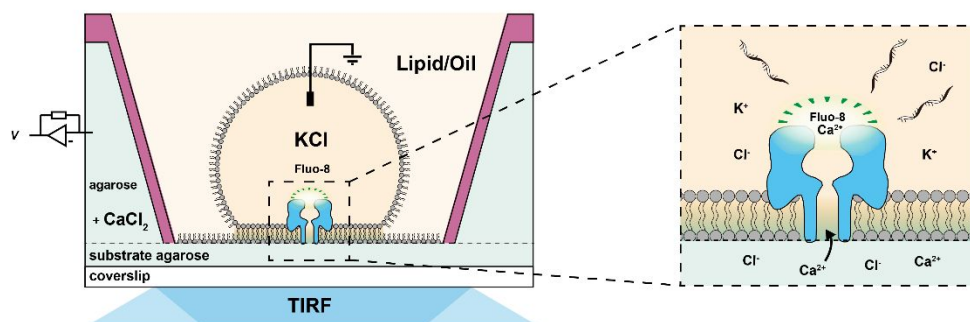


Figure S1. A DIB device. Left: the schematic diagram of a single DIB device. A 60× TIRF objective is used for both illumination and imaging. DIB is formed by placing an aqueous droplet (~200 nL) on an agarose substrate immersed in a lipid/oil solution. A voltage protocol is applied using Ag/AgCl electrodes placed respectively in the agarose substrate and the droplet. Right: a zoomed-in cartoon of oSCR of nucleic acid translocation. Ca^{2+} in the hydrogel migrates through the nanopore and binds with Fluo-8 in the droplet to form a complex. Upon TIRF illumination, the formed complex around the pore vicinity emits fluorescence, appearing as a fluorescence spot. When a strand of nucleic acid translocates through the pore, the pore is blocked, simultaneously blocking the transport of Ca^{2+} from *trans* to *cis*. Consequently, the fluorescence intensity became diminished, indicating the observation of a translocation event.

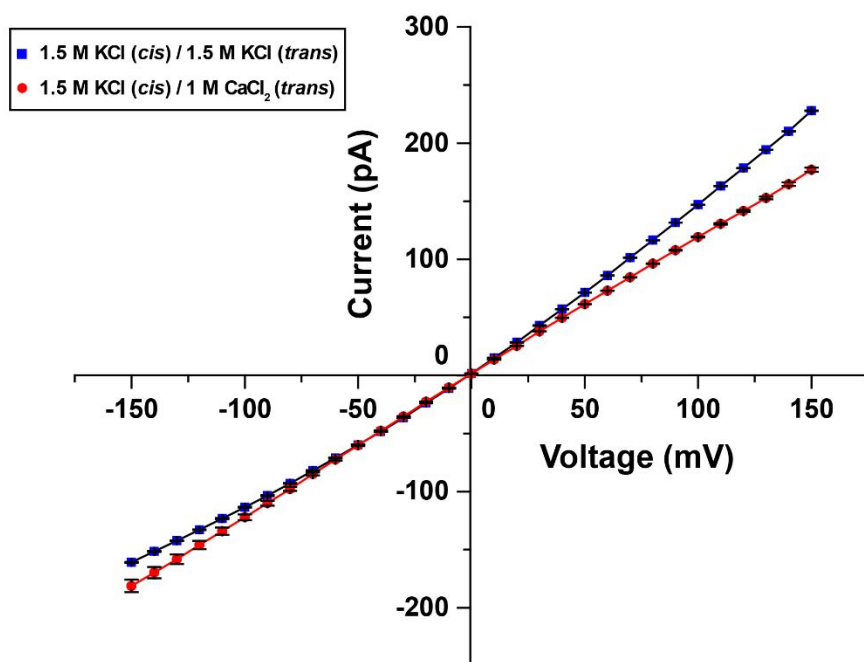


Figure S2. I-V curves of α -HL with different buffer combinations. Results of I-V curve measurements were acquired with different buffer combinations during electrophysiology measurements. No analyte was involved during the measurements. Error bars were based on three independent measurements (N=3). The presence of 1 M CaCl_2 instead of 1.5 M KCl in *trans* results in an obvious drop of open pore current, when a positive bias is applied.

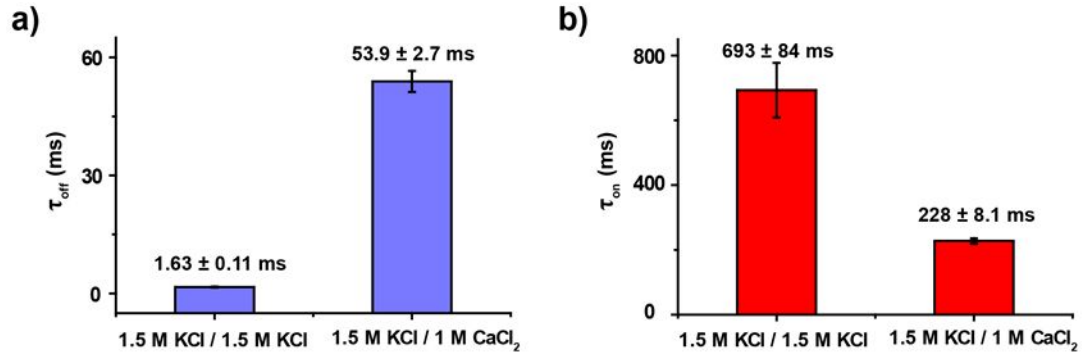


Figure S3. τ_{off} and τ_{on} of Let-7a translocation. The mean dwell time (τ_{off}) **a)** and the mean inter-event interval (τ_{on}) **b)** of Let-7a translocation events are demonstrated. Electrophysiology measurements were carried out with a buffer combination of either 1.5 M KCl/1.5 M KCl (*cis/trans*) or 1.5 M KCl/1.0 M CaCl_2 (*cis/trans*). Let-7a was added to the *cis* compartment with a 1.0 μM final concentration. A +100 mV potential was continuously applied. Error bars were based on three independent experiments (N=3).

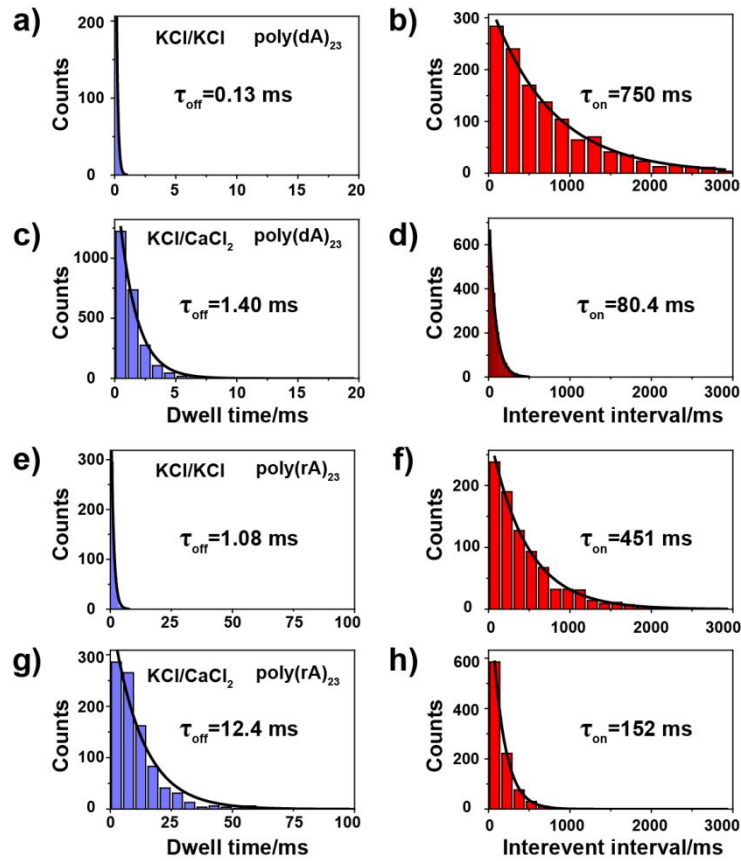


Figure S4. τ_{off} and τ_{on} of poly(dA)₂₃ and poly(rA)₂₃. Translocation of poly(dA)₂₃ or poly(rA)₂₃ was carried out with different combinations of electrolyte buffer. The buffer combination is denoted in the format of *cis/trans*. Here, the label KCl represents a buffer of 1.5 M KCl and 10 mM HEPES at pH 7.0. The label CaCl₂ represents a buffer of 1.0 M CaCl₂ and 10 mM HEPES at pH 7.0. Poly(dA)₂₃ or poly(rA)₂₃ was added to the *cis* side with a 1.0 μ M final concentration. A +100 mV potential was continuously applied. From the above demonstrated results, the reduction of the translocation speed and the increase of the capture rate were quantitatively verified, as demonstrated by the corresponding histograms **a-h**). Solid lines are single exponential fits to the histograms. τ_{off} and τ_{on} values were derived from the fitting results.

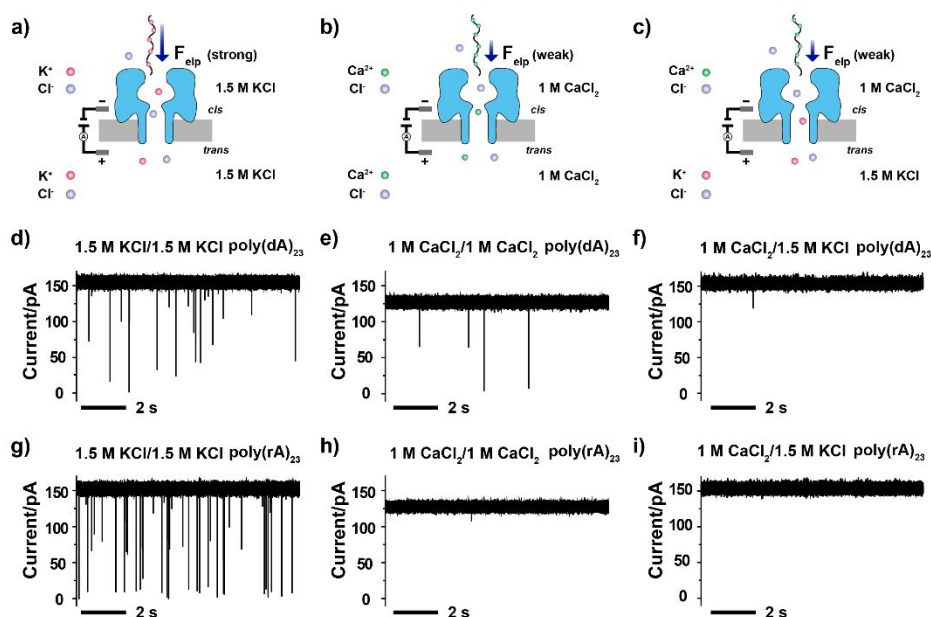


Figure S5. Electrophysiology measurements with CaCl_2 in *cis*. Translocation of poly(dA)_{23} or poly(rA)_{23} was carried out with different combinations of electrolyte buffer. The buffer combination is denoted in the format of *cis/trans*. Here, the label 1.5 M KCl represents a buffer of 1.5 M KCl and 10 mM HEPES at pH 7.0. Whereas, the label 1.0 M CaCl_2 represents a buffer of 1.0 M CaCl_2 and 10 mM HEPES at pH 7.0. Poly(dA)_{23} or poly(rA)_{23} was added to the *cis* side with a 1.0 μM final concentration. A +100 mV potential was continuously applied. **a-c)** Schematic diagram of nucleic acids translocation. Representative current traces of **d-f)** poly(dA)_{23} or **g-i)** poly(rA)_{23} translocation acquired with different buffer combinations. From this set of experiments, it is clearly conclusive that CaCl_2 should not be presented in *cis*, in which the nucleic acid analyte is also placed. The strong coupling between free Ca^{2+} and the nucleic acids has significantly reduced the effective charge on the nucleic acid analyte, which in turn has significantly reduced the appearance rate of nucleic acid translocation.

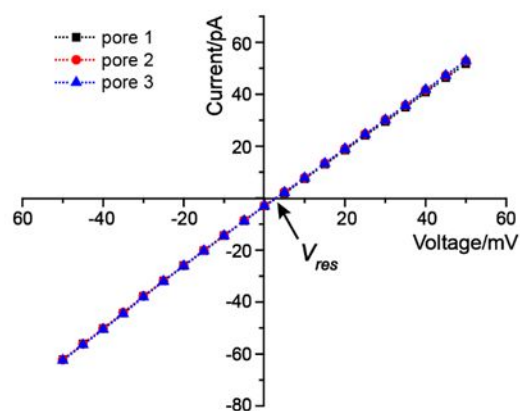


Figure S6. Reverse potential measurement. The nanopore measurement system is first electrically balanced when both sides of the chamber is filled with a 1.5 M potassium chloride buffer. The electrical balance is achieved when the measured current is 0 pA when the applied potential is 0 mV. Then the electrolyte buffer in *trans* is replaced with 1.0 M CaCl_2 and an I-V curve is measured. The reverse potential is derived from the I-V curve, as marked with V_{res} , of which the measured current is 0 pA. WT alpha hemolysin is used during the measurement.

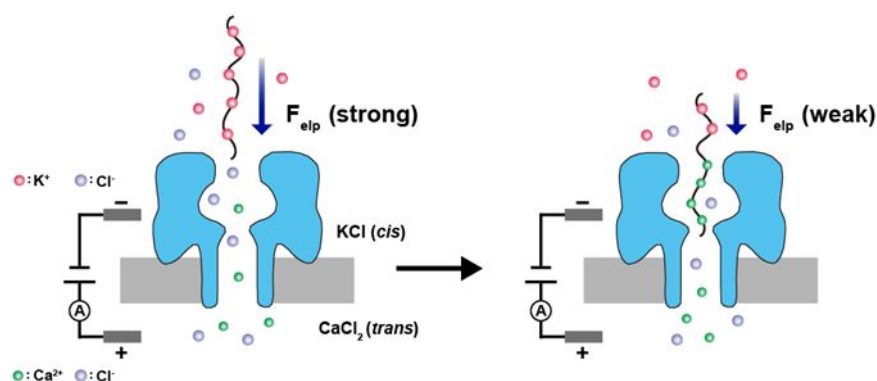


Figure S7. Retarded nucleic acid translocation in the presence of a calcium flux.

During electrophysiology measurements with an asymmetric buffer combination, a KCl buffer in *cis* and a CaCl₂ buffer in *trans*, retarded translocation of nucleic acids is observed. In this measurement condition, free Ca²⁺ distributes inhomogeneously around the pore vicinity in the form of a calcium flux. The nucleic acid, which is placed in *cis*, interacts weakly with K⁺, but still maintains enough net-negative charges which could be dragged by electrophoretic force (F_{elp}) for translocation. The increased concentration of Ca²⁺ competitively binds with the nucleic acid when it is dragged near the pore, and this further neutralizes the negative charges of the nucleic acid. As a result, the translocation speed is generally retarded and the capture rate is not reduced.

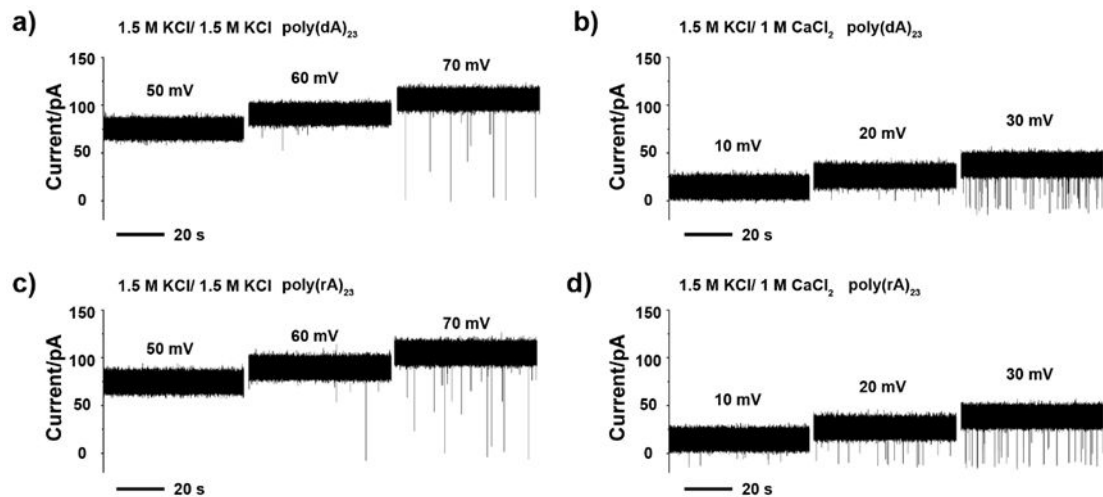


Figure S8. Reduced threshold voltage. The measurements were carried out with a fixed buffer of 1.5 M KCl and 10 mM HEPES at pH 7.0 in *cis* but with various buffers in *trans*. The buffer in *trans* was either 1.5 M KCl and 10 mM HEPES at pH 7.0 or 1.0 M CaCl₂ and 10 mM HEPES at pH 7.0, as labeled in the figures. Poly(dA)₂₃ or poly(rA)₂₃, which respectively act as representative DNA or RNA analytes, was added to the *cis* side with a 1.0 μ M final concentration. With a buffer combination of 1.5 M KCl/1.5 M KCl, a minimum applied voltage to efficiently drive **a**) poly(dA)₂₃ or **c**) poly(rA)₂₃ translocation is around 70 mV. However, with a buffer combination of 1.5 M KCl/1.0 M CaCl₂, the minimum applied voltage to efficiently drive **b**) poly(dA)₂₃ or **d**) poly(rA)₂₃ translocation was reduced to around 30 mV.

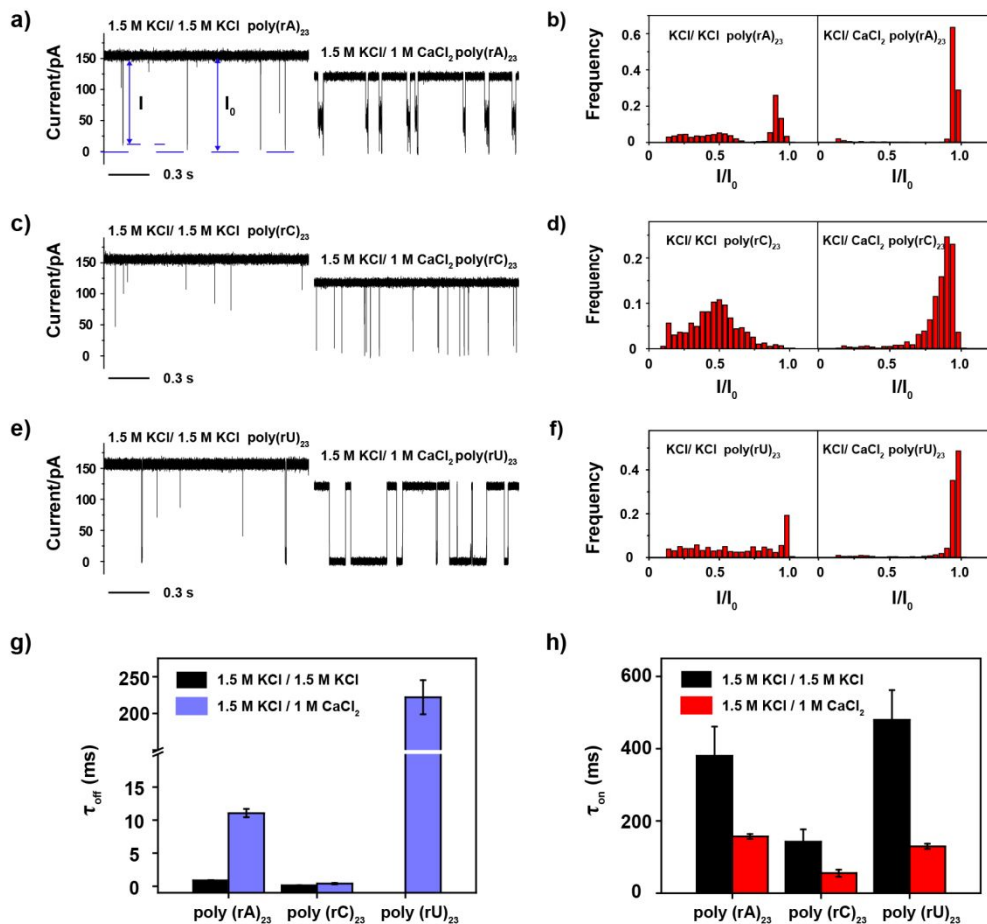


Figure S9. Translocation of RNA homopolymers under different conditions. The measurements were carried out with a fixed buffer of 1.5 M KCl and 10 mM HEPES at pH 7.0 in *cis* but with various buffers in *trans*. The buffer in *trans* was either 1.5 M KCl and 10 mM HEPES at pH 7.0 or 1.0 M CaCl₂ and 10 mM HEPES at pH 7.0, as labeled in the Figures. All measurements were recorded with a +100 mV applied potential. Representative current traces of **a)** poly(rA)₂₃, **c)** poly(rC)₂₃ or **e)** poly(rU)₂₃ with different electrolyte buffer combinations are demonstrated. The corresponding histograms of I/I_0 from measurements taken with **b)** poly(rA)₂₃, **d)** poly(rC)₂₃ or **f)** poly(rU)₂₃. **g)** Mean dwell times (τ_{off}) for poly(rA)₂₃, poly(rC)₂₃ and poly(rU)₂₃ measured with different electrolyte combinations. **h)** Mean inter-event intervals (τ_{on}) for poly(rA)₂₃, poly(rC)₂₃ and poly(rU)₂₃ measured with different electrolyte combinations. Each RNA homopolymer was added to the *cis* side with a 1 μ M final concentration. Error bars were based on three independent experiments (N=3).

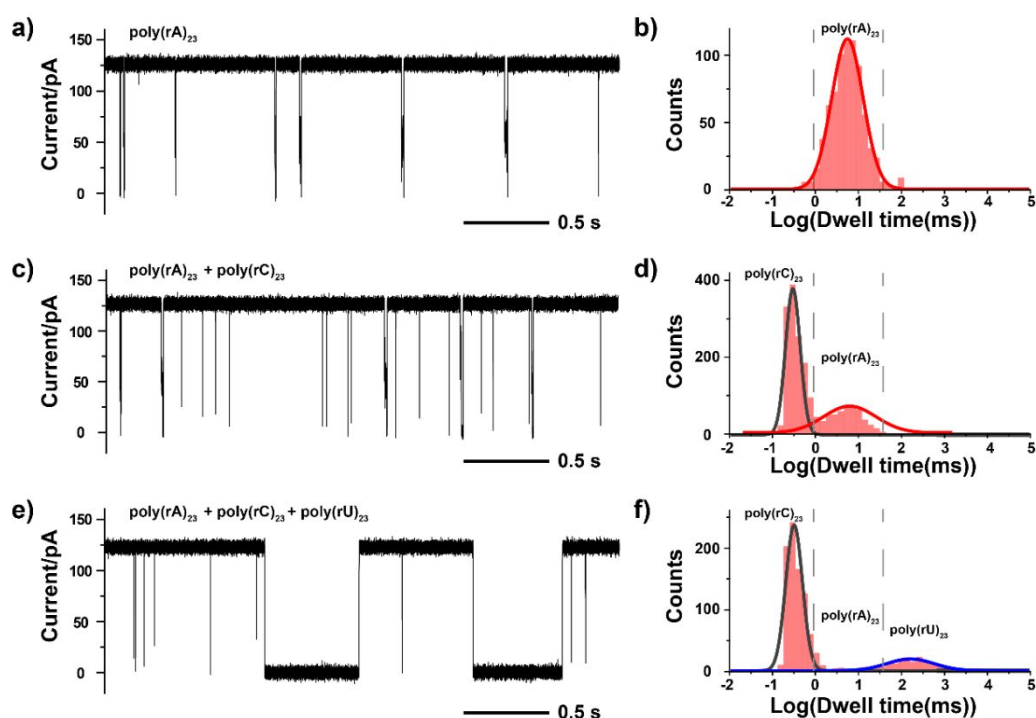


Figure S10. Simultaneous detection of RNA homopolymers. The measurement was carried out with a buffer combination of (1.5 M KCl and 10 mM HEPES at pH 7.0) in *cis* and (1 M CaCl_2 and 10 mM HEPES at pH 7.0) in *trans*. A constant +100 mV potential is applied. RNA homopolymers (poly(rA)_{23} , poly(rC)_{23} and poly(rU)_{23}) were sequentially added and simultaneously measured with the same pore. **a)** Representative traces acquired with poly(rA)_{23} . Only one type of translocation event were observed, as demonstrated from the trace and the histogram of $\log(\tau_{off})$ in **b**. **c)** The representative trace acquired with poly(rA)_{23} and poly(rC)_{23} . Clearly, two populations of events were observed from the trace and the histogram of $\log(\tau_{off})$ in **d**. **e)** The representative traces acquired with poly(rA)_{23} , poly(rC)_{23} and poly(rU)_{23} . Translocation of poly(rU)_{23} can be easily recognized by its extremely long dwell time. Only two populations of events can be clearly observed from the histogram of $\log(\tau_{off})$ in **f**. The disappearance of poly(rA)_{23} events in **f** is a consequence of spontaneous hybridization between poly(rA)_{23} and poly(rU)_{23} , when simultaneously present in the measurement buffer. Poly(rA)_{23} and poly(rC)_{23} were added to the *cis* side with a 0.25 μM final concentration for each composite. Poly(rU)_{23} was added with a 0.6 μM final concentration.

Table S1. Strand sequences.

Strand	Sequence (5'-3')
Let-7a	UGAGGUAGUAGGUUGUAUAGUU
poly(dA) ₂₃	d(AAAAAAAAAAAAAAAAAAAAAAAAAA)
poly(rA) ₂₃	r(AAAAAAAAAAAAAAAAAAAAAAAAAA)
poly(rC) ₂₃	r(CCCCCCCCCCCCCCCCCCCCCCCC)
poly(rU) ₂₃	r(UUUUUUUUUUUUUUUUUUUUUUU)

Table S2. τ_{off} and τ_{on} of poly(dA)₂₃ in different buffer combinations.

poly(dA) ₂₃	1.5 M KCl <i>trans</i>	1 M CaCl ₂ <i>trans</i>	2 M CaCl ₂ <i>trans</i>	3 M CaCl ₂ <i>trans</i>
τ_{off} (ms)	0.13±0.02	1.53±0.09	2.21±0.16	3.6±0.20
τ_{on} (ms)	627±104	80.7±8.6	34.4±5.9	22.0±1.8

The buffer in *cis* is 1.5 M KCl and 10 mM HEPES at pH 7.0. The buffer in *trans* is described in the table. Poly(dA)₂₃ was added to the *cis* side with a 1.0 μ M final concentration and a +100 mV potential was applied continuously.

Table S3. τ_{off} and τ_{on} of poly(rA)₂₃ in different buffer combinations.

poly(rA) ₂₃	1.5 M KCl <i>trans</i>	1 M CaCl ₂ <i>trans</i>	2 M CaCl ₂ <i>trans</i>	3 M CaCl ₂ <i>trans</i>
τ_{off} (ms)	0.88 ± 0.07	11.1 ± 0.63	15.0 ± 0.62	22.8 ± 0.67
τ_{on} (ms)	380 ± 81	157 ± 6.8	69.2 ± 8.0	48.1 ± 3.9

The buffer in *cis* is 1.5 M KCl and 10 mM HEPES at pH 7.0. The buffer in *trans* is described in the table. Poly(rA)₂₃ was added to the *cis* side with a 1.0 μ M final concentration and +100 mV potential was continuously applied.

Table S4. The ratio of effective translocation for RNA homopolymers.

	1.5 M KCl (<i>cis</i>)/1.5 M KCl (<i>trans</i>)	1.5 M KCl (<i>cis</i>)/1 M CaCl ₂ (<i>trans</i>)
poly(rA) ₂₃	(56.6 ± 8.4)%	(95.4 ± 2.6)%
poly(rC) ₂₃	(6.31 ± 1.6)%	(92.6 ± 1.9)%
poly(rU) ₂₃	(40.2 ± 3.6)%	(91.1 ± 2.4)%

RNA homopolymers were added to the *cis* side with a 1 μ M final concentration. The buffer

used was 10 mM HEPES at pH 7.0 and a +100 mV potential was continuously applied. Effective translocation is defined as events with a deep enough percentage blockage ($I/I_0 > 70\%$).

Table S5. τ_{off} and τ_{on} of RNA homopolymers translocation.

	1.5 KCl (<i>cis</i>) / 1.5 M KCl (<i>trans</i>)		1.5 M KCl (<i>cis</i>) / 1 M CaCl ₂ (<i>trans</i>)	
	τ_{off} (ms)	τ_{on} (ms)	τ_{off} (ms)	τ_{on} (ms)
poly(rA) ₂₃	0.88 ± 0.07	380 ± 81	11.1 ± 0.63	157 ± 6.8
poly(rC) ₂₃	0.12 ± 0.03	142 ± 34	0.39 ± 0.10	55.4 ± 9.7
poly(rU) ₂₃		480 ± 82	222 ± 23	130 ± 7.3

RNA homopolymers were added to the *cis* side with a 1 μ M final concentration. The buffer used was 10 mM HEPES at pH 7.0 and a +100 mV potential was continuously applied.